USE OF ACOUSTIC EMISSION TO MONITOR PROGRESSIVE DAMAGE ACCUMULATION IN KEVLAR® 49 COMPOSITES

J. M. Waller[1], R. L. Saulsberry[2], and E. Andrade[3]

[1]Materials Scientist, NASA Johnson Space Center White Sands Test Facility, Laboratories Department, MS 200LD, Las Cruces, New Mexico 88011
[2]Project Manager, NASA Johnson Space Center White Sands Test Facility, Laboratories Department, MS 200LD, Las Cruces, New Mexico 88011.
[3]USRP Intern, Department of Metallurgical and Materials Engineering, University of Texas at El Paso, Texas 79968

ABSTRACT. Acoustic emission (AE) data acquired during intermittent load hold tensile testing of epoxy impregnated Kevlar® 49 (K/Ep) composite strands were analyzed to monitor progressive damage during the approach to tensile failure. Insight into the progressive damage of K/Ep strands was gained by monitoring AE event rate and energy. Source location based on energy attenuation and arrival time data was used to discern between significant AE attributable to microstructural damage and spurious AE attributable to noise. One of the significant findings was the observation of increasing violation of the Kaiser effect (Felicity ratio < 1.0) with damage accumulation. The efficacy of three different intermittent load hold stress schedules that allowed the Felicity ratio to be determined analytically is discussed.

Keywords: Acoustic emission; nondestructive evaluation; Kaiser effect; Felicity ratio; COPV
PACS: 43.40.Le Techniques for nondestructive evaluation and monitoring, acoustic emission

INTRODUCTION

Composite Overwrapped Pressure Vessels (COPVs) are widely used in launch vehicles and satellites, where the strong drive to reduce weight has pushed COPV designers to adopt high performance, high specific strength composite materials with a relatively high volume fraction ($v_f \approx 0.6$ to 0.7) of fiber. To date, the composite materials used in COPV designs have typically consisted of aramid or carbon fiber embedded in a thermoset matrix such as epoxy. The role of the matrix is to transfer pressurization load to the fiber, while the role of the fiber is to withstand the load over time under the environmental exposure conditions encountered in service. Pressurizations on the order of 350 to 700 bar (5000 to

10,000 psi) are common for COPVs. This has necessitated the use of high load bearing composite overwraps wound around a thin-walled metal liner.

NASA has been faced with recertification and life extension issues for epoxy impregnated Kevlar® 49 (K/Ep) COPVs distributed throughout various systems on the Space Shuttle Orbiter. The Shuttle COPVs have varying criticality, usage histories, damage and repair histories, time at pressure, and number of pressure cycles. The original certification for Shuttle COPVs was for 10 years, which was later extended to 20 years. Currently, Shuttle COPVs operating without certification are being flown on waiver. Also, K/Ep COPVs like those used on the Shuttle are of particular concern due to the insidious and catastrophic "burst-before-leak" (BBL) failure mode caused by stress rupture (SR) of the composite overwrap. SR life has been defined by the American Institute for Aeronautics and Astronautics (AIAA) Aerospace Pressure Vessels Standards Working Group as "the minimum time during which the composite maintains structural integrity considering the combined effects of stress level(s), time at stress level(s), and associated environment" [1]. SR has none of the features of predictability associated with metal pressure vessels, such as crack geometry, growth rate and size, or features that lend themselves to the use of nondestructive evaluation (NDE) methods. In essence, the variability or "surprise factor" associated with SR in K/Ep COPVs cannot be eliminated.

For these reasons, NASA has devoted much effort to develop NDE methods that can be used during post-manufacture qualification, in-service inspection, and in situ structural health monitoring. One of the more promising NDE techniques for detecting and monitoring, in real-time, the strain energy release and corresponding stress-wave propagation produced by actively growing flaws and defects in composite materials is acoustic emission (AE) [2, 3, 4, 5, 6, 7, 8, 9]. It is hoped that the procedures described in this paper lay the groundwork for establishing critical thresholds for accumulated damage in composite structures such as COPVs so that precautionary or preemptive engineering steps can be implemented to minimize or obviate the risk of catastrophic failure of those structures.

EXPERIMENTAL

Tensile Tester

Programmed tensile stress schedules were applied using an Instron® 5569 Series Electromechanical Test Instrument equipped with a 50 kN (11,200 lb_f) capacity load cell. Other features included self-tightening 25 × 50 mm (1 × 2 in.) wedge action mechanical grips, and a Windows compatible Bluehill® (version 1.8.289). To minimize excessive AE during loading and unloading ramps, a 20 N/min (4.5 lb_f/min) loading/unloading rate was used, consistent with the ASTM E 1118 [10] recommendation that the load rate should not exceed 5 percent per minute of the desired highest stress (in this case, the ultimate tensile strength (UTS)). To prevent saturation of the Bluehill® data acquisition buffer, a 1 to 2 s^{-1} data acquisition rate was used, depending on the duration of test (tests generally took 7 to 16 h to complete). Real-time stress and strain data were recorded during all tests. Tensile test data acquisition was synchronized with AE data acquisition (see next section) to facilitate monitoring of progressive damage accumulation as a function of applied stress.

Acoustic Emission

AE measurements were taken using a DWC FM-1 (Digital Wave Corp., Centennial, CO) system equipped with 8-channel capability, four of which were used in this study. Each channel was connected to a DWC PA-0, 0 dB gain preamplifier, and then to a broadband, high fidelity B1080 piezoelectric sensor with a frequency range of 1 kHz to 1.5 MHz (output signals were noisy and nonlinear at the lower 1 to 200 kHz end of the claimed frequency response range). The AE system was supported with a lunchbox computer equipped with WaveExplorer™ software (version 6.2.0). The software allowed arrival time, event energy, and event time to be acquired for all registered events. Sensor sensitivity was checked using pencil lead breaks performed midway between adjacent sensors, according to guidelines described in ASTM E 976 [11].

Materials

Unidirectional 4560 denier Kevlar® 49 composite strands (ca. 1987, received from Texas Research Institute (TRI), Austin, TX) had a UTS of 1312 ± 67 N (295 ± 15 lb_f) and an ultimate percent elongation (ε^*) of 3.1 ± 0.2 percent. The density of the Kevlar® was 144 kg/m³. Each tensile specimen was prepared per ASTM D 2343 [12] and had elliptical cross-sectional areas of 0.347 mm^2 (0.000544 in^2), with a nominal thickness of 1.1 mm (0.043 in.), width of 1.4 mm (0.055 in.), and a gauge length of 25 cm (10 in.). Each specimen had cardboard end tabs with a $l \times w = 5 \times 2.5$ cm (2 × 1 in.). Tow ends were secured to the cardboard with a bead of adhesive. Specimens were mounted vertically with sensors positioned approximately 5 cm (2 in.) from each other and the cardboard tabs (Fig. 1).

Load Schedules

Three different stress schedules were used. The first two schedules were based on the pressure tank examination procedure described in ASTM E 1067 [13], similarly referred to as the manufacturer's qualification test in ASTM E 1118 [10]. The load sequence began with an initial hold period between 10 and 30 min to determine the level of spurious AE attributable to background noise as the specimen was held in an unloaded state. These two procedures will be described generically as intermittent load-hold (ILH) stress schedules in this paper, and more specifically as ILH1 and ILH2 (Table 1, Figures 2 and 3, respectively).

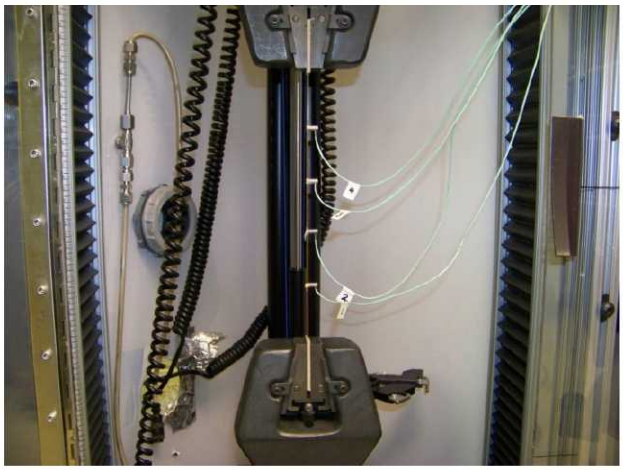

FIGURE 1. 4560 denier K/Ep tow (25 cm gauge length) aligned in grips showing four B1080 AE sensors mounted.

TABLE 1. Description of Intermittent Load-Hold Stress Schedules

ILH1	ILH2
1. Ramp: Load to 530 N (120 lb_f)	1. Ramp: Load to 890 N (200 lb_f)
2. 10-min load hold	2. 15-min load hold
3. Ramp: Unload 90 N (20 lb_f)	3. Ramp: Unload 22 N (5 lb_f)
4. 10-min hold	4. 15-min hold
5. Ramp 220 N (50 lb_f) to next highest load	5. Ramp 53 N (12 lb_f) to next highest load
6. Repeat Steps 2-5 until UTS is reached	6. Repeat Steps 2-5 until UTS is reached

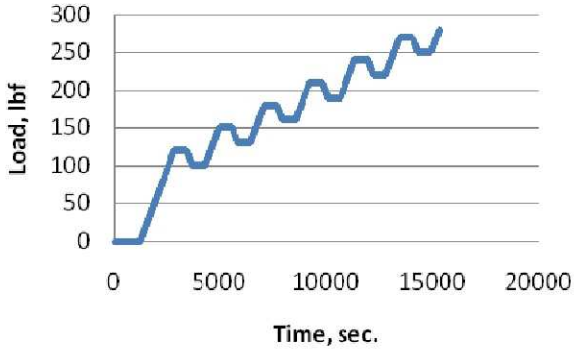

FIGURE 2. Representative intermittent load-hold (ILH) stress schedule used for K/Ep tow characterization (ILH1, based on ASTM E 1067 and E 1118)

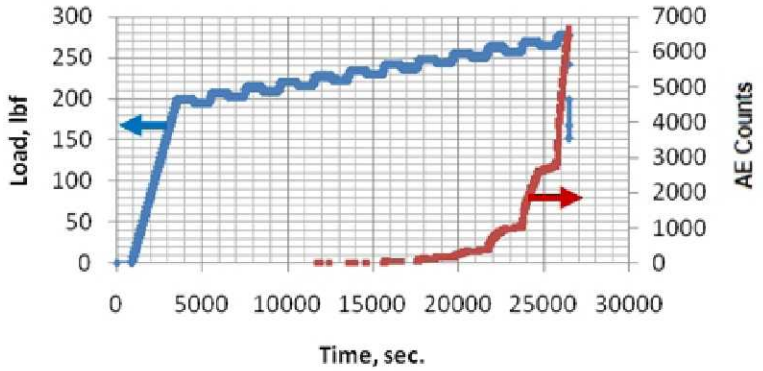

FIGURE 3. Nonlinear increase in significant AE (red data) during an intermittent load hold (ILH2) stress schedule test (blue data)

The ILH1 method encompassed stresses between 530 N (120 lb_f) and rupture at approximately 1250 N (280 lb_f), and allowed the onset of the first significant AE to be determined. The ILH2 method was developed to impose more load-holds between the region where significant AE was first observed (around 890 N (200 lb_f)) and rupture, in order to yield more information about the damage evolution closer to rupture. The 53:22 N (2.41:1) loading:unloading ratio used in the ILH2 method was nearly identical to the 220:90 N (2.44:1) loading:unloading ratio used in the ILH1 method (Steps 3 and 5, Table 1).

One of the established tenets describing AE states that if a material is loaded, unloaded, and then reloaded, new AE activity will not occur until the highest load previously experienced by the material is exceeded. This phenomenon is known as the Kaiser effect, and is observed in materials that behave elastically during reloading (i.e., have undergone negligible plastic or permanent deformation (viscous loss processes) during previous loadings). However, once damage begins to accumulate in fiber reinforced polymer (FRP) materials, the Kaiser effect begins to be violated and new AE activity will occur in subsequent loadings (or COPV pressurizations) before the highest previous load (or pressure) is reached. The analytical parameter that describes departure from the Kaiser effect is known as Felicity ratio (FR) which is given by:

FR = stress level where AE begins in load cycle / maximum previous stress

When FR $\geq$ 1.0, the Kaiser effect is said to be followed, while for FR $<$ 1.0, the Kaiser effect is said to be violated. Also, the larger the departure of the FR at a value less than unity, the more pronounced the accumulated damage. Damage accumulation trends as revealed by FR data have been well documented in AE studies on concrete [14], and are a centerpiece of ASTM standards used for AE qualification of FRP materials [10, 13]. Both the ILH1 and ILH2 procedures were found to be useful in detecting violations of the Kaiser effect.

The Japanese Society for Non-Destructive Inspection (JSNDI) developed an alternate stress schedule successfully used to characterize concrete failure [15]. Like the ILH1 and ILH2 methods, the Japanese practice detects violations of the Kaiser effect through measurement of the FR, but proposes another index value for assessing accumulated damage: namely, the calm ratio (CR). Unlike the FR, the CR is attributable to the occurrence of significant AE during *un*loading cycles, but in situations where the FR

< 1.0, is also indicative of accumulated damage. Analytically, the CR is determined using the expression:

CR = accumulated AE events during the unloading portion of a stress schedule / accumulated events during the preceding loading cycle

The Japanese practice has been successfully used by Lovejoy [14] to assess the severity of damage in concrete. In this method, denoted ILH3, the FR and CR are plotted against stress, and the intersection point of the linear least squares fits determined, to give the critical CR threshold below which incipient or intermediate damage occurs and above which intermediate or severe damage occurs. Application of the ILH3 stress schedule (Fig. 4) to K/Ep gave an opportunity to test the validity of JSNDI approach (Standard unavailable) to a fiber reinforced composite material. It is unknown to what extent analytical procedures for CR determination have been applied to FRP materials.

RESULTS AND DISCUSSION

Acoustic Emission Data Reduction

Background noise checks were performed before each programmed stress schedule to determine the level of spurious AE. Typical characteristics of spurious AE were: 1) low energy (< 0.5 V^{2}-μs), and 2) indeterminate source location as revealed by 0, 1 or 2 arrival times. Such events were categorized by the WaveExplorer™ software as having a

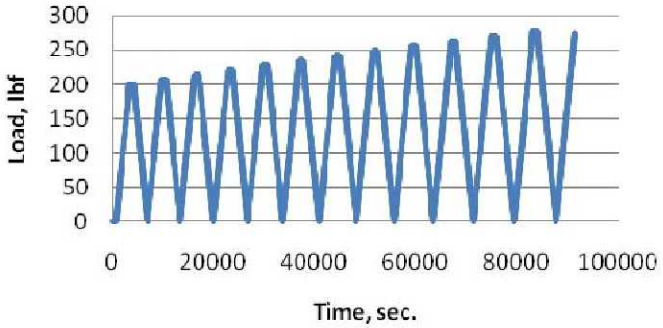

FIGURE 4. Representative intermittent load-hold (ILH) stress schedule used for K/Ep tow characterization (ILH3, based on NDIS 2421 [16])

nonsensical zone location = -1. Further verification that suspected spurious AE events were actual background noise was obtained by showing that the background AE event rate did not change with respect to the applied stress schedule (Fig. 5). Further analysis of the AE background data revealed a nearly constant background count rate equal to about 1.8 counts/min during successive (Step 5, Table 1) ILH1 plateaus of increasing applied stress, offering further verification that the AE events such as depicted in Fig. 5 were spurious.

Once spurious AE was removed from the data sets, AE events indicative of probable grip noise were identified. Typical characteristics of grip noise were: 1) low energy (< 0.7 V^{2}-μs), and 2) first arrival times at either sensor 1 or 4 as revealed by trending arrival time data at two or more sensors (for example, $t_1 < t_2$ ($< t_3 < t_4$) for grip noise originating in the grip closest to sensor 1, or conversely, $t_1 > t_2$ ($> t_3 > t_4$) for grip noise

originating in the grip closest to sensor 4). AE events detected only at sensor 1 or 4 (only t_1 or t_4 existed), and meeting the above < 0.7 V^2-μs energy requirement, were also categorized as grip noise. Qualitatively, the AE signature of grip noise was indistinguishable from that of spurious background noise. A more thorough arrival time, energy, and frequency analysis is underway to further differentiate between valid low energy grip noise, and low energy events that may have been attributable instead to matrix cracking, debonding, and pull-out that occurred closest to sensors 1 and 4.

Additional details of the data filtering process were as follows. The 0.5 V^2-μs low energy threshold for spurious background AE was calculated by averaging all the energies measured at the first arrival channel. AE events with energies that exceeded this threshold were examined using source location. All events that were determined to originate outside gauge length (grip noise) were removed from the data set, while all events that were determined to originate within the gauge length were retained (gauge events of interest, Fig. 6, top and bottom). Events that did not register source location data (only 1 or 2 arrival times observed) were then analyzed using energy distribution. First, each channel's energy was compared to the 0.5 V^2-μs threshold. Each channel 1-4 had to exceed a fixed threshold equal to 25 percent of the average energy above the average energy of the channel. Events that did not exceed the threshold were removed from the data set. Due to the proximity of sensors 1 and 4 to the grips, channels 2 and 3 were then analyzed according to their energies. These channels had to exceed a fixed threshold equal to 25 percent of the maximum energy for spurious background AE above the average energy at each specified channel. The events that exceeded this threshold were then combined with the source locatable events and were then renumbered relative to time.

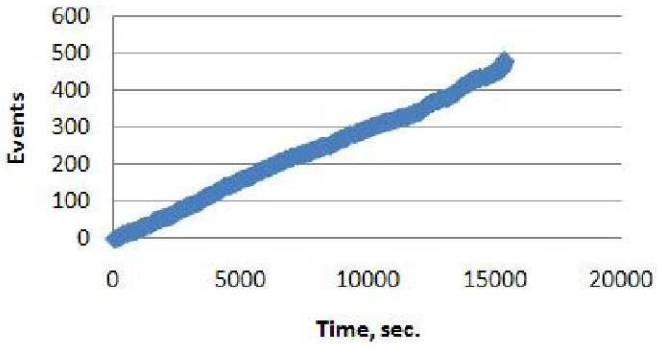

FIGURE 5. Cumulative background AE during a intermittent load hold (ILH1) stress schedule test

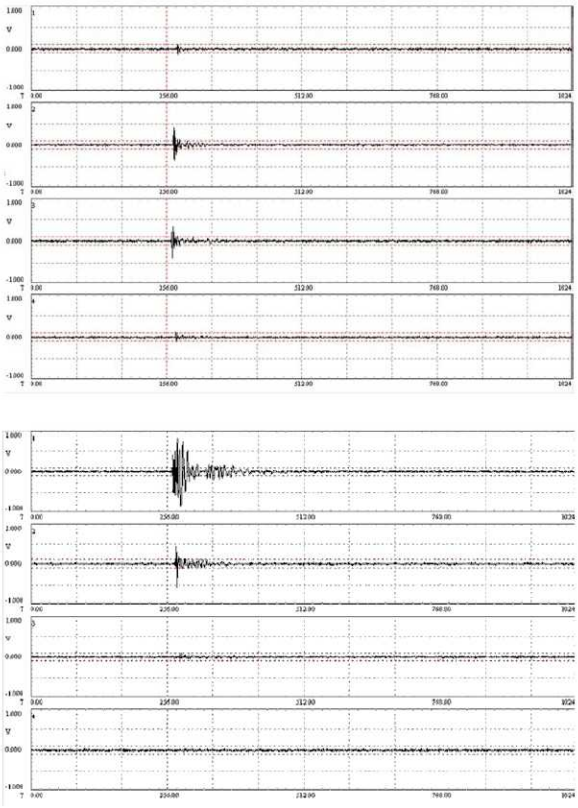

FIGURE 6. Significant AE events occurring in the gauge region at stresses where significant AE was first observed (top, t = 11,270 s), and a more energetic event close to one of the grips at a later time (bottom, t = 13,984 s), for a K/Ep tensile specimen subjected to an intermittent load hold (ILH2) stress schedule

Acoustic Emission Data Interpretation

Significant, source-locatable AE that exceeded the energy threshold screening criteria and also originated in the gauge region of the specimen (Fig. 6) were found to occur at loads above 890 N (200 lb_f), which corresponds to an elapsed time greater than 11,000 s in the ILH2 method (Fig. 3). Another feature observed was a dramatic increase in the AE count rate as failure was approached (Fig. 3). Nonlinear increases in the AE event rate are described in ASTM E 1067 and E 1118 as corresponding to regions of critically intense AE activity indicative of accumulated, severe damage. Also of note is the fact that these regions also show the greatest violation of the Kaiser effect and, therefore, the lowest FR values. Similarly, the highest CRs should be observed in such regions.

Strain data are also known to correlate with AE data and give a fair indication of the proximity of failure. In fact, studies have shown that the strain rate in creep tests reaches a minimum about two-thirds the way to failure in specimens held at constant stress [16]. Other investigators have shown that outbursts of AE activity often coincide with discontinuous changes in strain [17]. However, for purposes of this investigation, it was sufficient to show that the ultimate strain was in agreement with published values. For example, an ultimate percent strain of about 3.5 percent was observed in the ILH2 stress schedule test, which compared favorably to the expected TRI value of 3.1 ± 0.2 percent.

The slightly higher ultimate percent strain may be due to specimen age since last tested (tested at TRI in 2006), or the ILH stress schedule used here versus the tensile test used by TRI.

Felicity Ratio Interpretation

The most significant finding of the present investigation was the linear decrease in the FR with increasing stress during the ILH1 method (Fig. 7, duplicate data), and the ILH2 method (Fig. 8). The correlation coefficients for the ILH methods indicated good ($R^2 = 0.866$) to excellent ($R^2 = 0.985$) agreement. The duplicate agreement obtained in the ILH1 method is also instructive. Taking FR = 1 as the threshold for significant accumulated damage, stress thresholds of 1054 N (237 lb_f) were obtained in both cases. The ILH2 method, despite its poorer correlation coefficient, predicted an onset of significant damage in the vicinity of 1070 N (240 lb_f). This remarkable agreement suggests that COPV materials-of-construction (namely, K/Ep and C/Ep tows), and COPVs themselves, could be qualified using ILH-type stress schedules to identify the specific point in a test specimen's accumulated stress history beyond which accumulated damage begins to occur. Also, since stress and time are nearly equivalent from a physical aging standpoint, accelerated test methodologies could be developed whereby elevated stress schedules could be used to predict the threshold of significant damage occurring at lower stress (i.e., operational COPV pressures, subjected to creep loading for prolonged periods of time).

Examination of AE energies also gave a similar indication of accumulated damage (data not shown). At the FR = 1.0 threshold, quite energetic events in excess of 10 V^2-μs began to be observed. It is presently unknown if such events are indicative of fiber rupture. Efforts are presently underway to look at the frequency of these high energy events, since fiber rupture is expected to occur above 300 to 400 kHz. The broadband sensors used in this study should be ideally suited for picking up damage signatures in this frequency range.

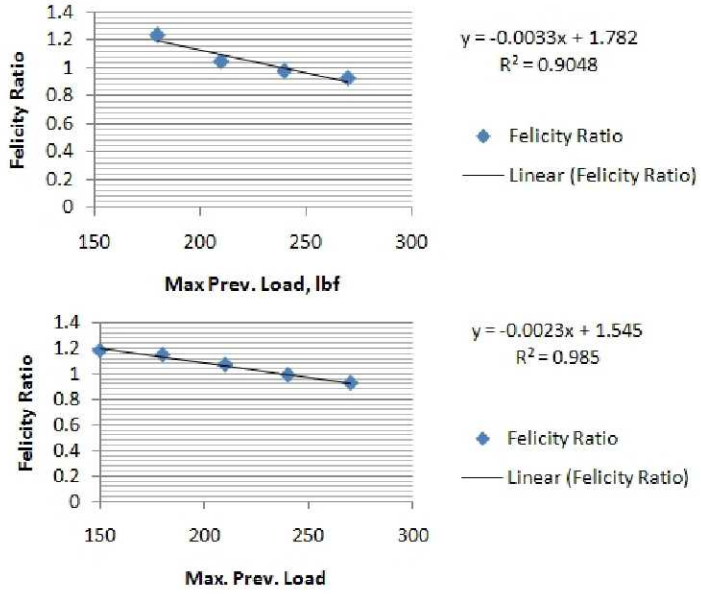

FIGURE 7. Dependence of Felicity ratio on stress during an intermittent load hold (ILH1) stress schedule test (duplicate results).

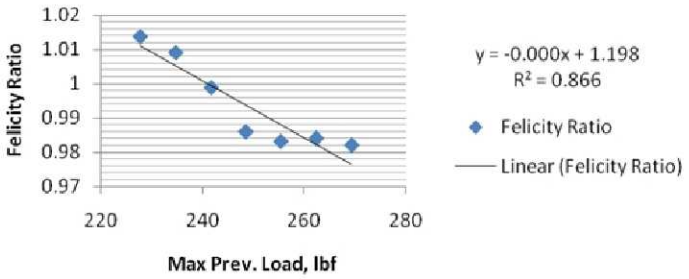

FIGURE 8. Dependence of Felicity ratio on stress during an intermittent load hold (ILH2) stress schedule test.

Calm Ratio Interpretation

CRs were not observed during the ILH1, or strangely enough, during the ILH3 stress schedules. However, in the ILH2 case (data not shown), there was enough AE activity during unloading portions of the test to obtain a measurable CR, so that a linear least squares fit to the data could be made, and the intersection point of the linear least squares CR and FR fits determined, to give the critical CR threshold, below which incipient or intermediate damage occurred and above which intermediate or severe damage occurred. Development of optimized stress schedules may allow greater exploitation of CR data and allow quantitative thresholds for incipient, moderate, and severe damage to be determined for composite materials such as K/Ep and C/Ep.

SUMMARY

The Felicity ratio was found to give a reproducible estimate of the stress threshold at which significant accumulated damage began to occur. Further refinement of stress schedules for determining Felicity ratio and Calm ratio could lead to robust pass-fail acceptance criteria once the type, level, and significance of the accumulated damage is better understood. This, in turn, will entail further reduction of the available or future AE data sets to determine what precursor events are operative and when, and how much of a given precursor event can be tolerated. That said, one observation stands out clearly: violation of the Kaiser effect (FR < 1.0) is paramount in assessing K/Ep damage and, therefore, in assessing damage in K/Ep overwraps. Future work is planned to ascertain the actual types of microscopic damage occurring at and below the FR = 1.0 threshold, as well as the efficacy of using the intermittent load hold stress schedule approach toward determining damage thresholds in C/Ep.

ACKNOWLEDGMENTS

The authors are grateful to Shawn Arnette of TRI (Austin, TX) for supplying K/Ep test specimens, and to Paul Spencer and Ben Gonzalez (NASA White Sands Test Facility) for assistance with setting up the universal tensile tester. Ongoing efforts at WSTF to

develop AE methods specific to K/Ep and C/Ep have been sponsored by the Office of Safety and Mission Assurance Office, NASA, Washington, DC.

REFERENCES

1. AIAA S-081A-2006, *Space Systems – Composite Overwrapped Pressure Vessels (COPVs),* American Institute of Aeronautics and Astronautics, Reston, VA (2006).
2. J. Awerbuch and S. Ghafari, "Monitoring Progression of Matrix Splitting During Fatigue Loading Through Acoustic Emission in Notched Unidirectional Graphite/Epoxy Composites," *J. Reinforced Plastics and Composites*, **7,** pp. 245-263 (1988).
3. T. Ely and E. Hill, "Longitudinal Splitting and Fiber Breakage Characterization in Graphite Epoxy Using Acoustic Emission Data," *Matl. Eval*., 288-294 (1995).
4. P. De Groot, P. Wijnen, and R. Janssen, "Real-time Frequency Determination of Acoustic Emission for Different Fracture Mechanisms in Carbon/Epoxy Composites," *Composites Sci. Technol.*, **55**, pp. 405-421 (1995).
5. W. H. Prosser, K. E. , Jackson, S. Kellas, B. T. Smith, J. McKeon, and A. Friedman, "Advanced, Waveform Based Acoustic Emission Detection of Matrix Cracking in Composites," *Matls. Eval.*, **53**:9, pp. 1052-1058 (1995).
6. M. Shiwa, S. Carpenter, and T. Kishi, "Analysis of Acoustic Emission Signals Generated during the Fatigue Testing of GFRP," *J. Composite Matls*., **30**:18, pp. 2019-2041 (1996).
7. El Guerjouma, J.-C. Baboux, D. Ducret, N. Godin, P. Guy, S. Huguet, Y. Jayet, and T. Monnier, "Non-Destructive Evaluation of Damage and Failure of Fibre Reinforced Polymer Composites Using Ultrasonic Waves and Acoustic Emission," *Adv. Eng. Matl.*, **3**:8, pp. 601-608 (2001).
8. S. Huguet, N. Godin, R. Gaertner, L. Salmon, and D. Villard, "Use of Acoustic Emission to Identify Damage Modes in Glass Fibre Reinforced Polyester," *Composites Sci Technol.*, **62**, pp. 1433-1444 (2002).
9. Y. A. Dzenzis and J. Qian, "Analysis of Microdamage Evolution Histories in Composites," *Int. J. Solids and Structures*, **38**, pp.1831-1854 (2001).
10. ASTM E 1118, *Standard Practice for Acoustic Emission Examination of Reinforced Thermosetting Resin Pipe (RTRP),* American Society for Testing and Materials, West Conshohocken, PA (2005).
11. ASTM E 976, *Guide for Determining the Reproducibility of Acoustic Emission Sensor Response*, American Society for Testing and Materials, West Conshohocken, PA (2005).
12. ASTM D 2343, *Test Method for Tensile Properties of Glass Fiber Strands, Yarns, and Rovings Used in Reinforced Plastics,* American Society for Testing and Materials, West Conshohocken, Pennsylvania (2008).
13. ASTM E 1067, *Standard Practice for Acoustic Emission Examination of Fiberglass Reinforced Plastic Resin (FRP) Tanks/Vessels*, American Society for Testing and Materials, West Conshohocken, PA (2007).

14. S. Lovejoy, "A General Overview of Acoustic Emission Testing and it's Applications to Highway Infrastructure," Northwest Transportation Conference, Oregon Department of Transportation (2008).
15. NDIS 2421, *Recommended Practice for In Situ Monitoring of Concrete Structures by Acoustic Emission,* Japanese Society for Non-Destructive Inspection (2000).
16. D. Sornette, "Statistical Physics of Rupture in Heterogeneous Media," *J. Mech. Phys. Solids*, (http://arXiv.org/abs/condmat/0409524 (accessed June 30, 2009) (2005).
17. J. Waller and R. Saulsberry, "In-Situ NDE Characterization of Kevlar and Carbon Composite Micromechanics for Improved COPV Health Monitoring," NASA NDE Working Group website, http://nnwg.org/current/ (accessed June 30, 2009), under White Sands Test Facility (2008).